

Superimposed contributions to two-terminal and nonlocal spin signals in lateral spin-transport devices

R. Jansen,¹ A. Spiesser,¹ Y. Fujita,^{1,2} H. Saito,¹ S. Yamada,³ K. Hamaya,³ and S. Yuasa¹

¹Research Center for Emerging Computing Technologies, National Institute of Advanced Industrial Science and Technology (AIST), Tsukuba, Ibaraki, 305-8568, Japan

²Research Center for Magnetic and Spintronic Materials, National Institute for Materials Science (NIMS), Tsukuba, Ibaraki 305-0047, Japan

³Center for Spintronics Research Network, Graduate School of Engineering Science, Osaka University, Toyonaka 560-8531, Japan



(Received 12 August 2021; revised 5 October 2021; accepted 12 October 2021; published 22 October 2021)

The spin voltages produced by spin accumulation and Hanle spin precession in a lateral spin-transport device with a silicon channel and ferromagnetic tunnel contacts (Fe/MgO) are probed for a wide range of magnetic fields. Signal analysis reveals that for the interpretation of the two-terminal magnetoresistance and the nonlocal spin signals, one needs to consider various superimposed contributions, namely, (i) spin signals arising from spin transport of mobile carriers through the Si channel from one ferromagnetic contact to the other, thus depending on the relative magnetization of the two contacts, (ii) spin signals also arising from the spin accumulation of mobile carriers in the Si channel but generated at each of the ferromagnetic contacts separately, and (iii) spin signals originating from spin accumulation of carriers that are confined at or near the Si/MgO interface of the magnetic tunnel contacts, with rather different spin precession characteristics. Perhaps surprisingly, in the *nonlocal* spin signal a clear broad Hanle signal from confined electrons is also observed, and argued to be mediated by heat flow from the injector to the nonlocal detector.

DOI: [10.1103/PhysRevB.104.144419](https://doi.org/10.1103/PhysRevB.104.144419)

I. INTRODUCTION

Spintronics [1–4] is based on the generation, detection, and manipulation of spin current, the flow of spin angular momentum. Spin currents occur in ferromagnetic (FM) materials, can traverse interfaces between different classes of materials, and can also be induced in paramagnetic or diamagnetic materials and transported through them over distances that in many cases exceed a micron. For the study of spin currents in non-FM materials, lateral spin-transport devices [5–26] have been instrumental. Such devices consist of a lateral non-FM channel that is typically contacted by two FM electrodes and by some additional nonmagnetic electrodes. The FM contacts, which can be direct or include a tunnel barrier, enable the injection of a spin current into the channel, as well as the detection of the induced nonequilibrium spin density in the channel. These lateral spin-transport devices are mainly operated in two standard modes. The first is the nonlocal geometry [5–13], which uses four electrodes (two FM and two normal metal ones), thereby allowing the separation of the electrical charge current and the spin current. The second is the two-terminal geometry [14–26], which uses only the two FM contacts to apply the current and detect the spin voltage.

The nonlocal and two-terminal spin signals in lateral spin-transport devices are probed under the application of an external applied magnetic field, which can reverse the magnetization direction of the FM contacts or induce spin precession if the field is perpendicular to the spins. In most cases, the applied magnetic fields do not exceed a few 100 Oe, since this is sufficient to reverse the in-plane magnetization of a thin

FM strip, while it is also sufficient to induce spin precession and thereby suppress the spin accumulation in materials with a spin-relaxation time of the order of a nanosecond or larger. For the analysis of the resulting spin signals, one typically only considers the spins of electrons that are transported through the channel from the injector to the detector by spin diffusion, while for the 2T geometry, spin drift [27–30] also needs to be included. Here, we reexamine the spin signals in a lateral spin transport device with a Si channel and Fe/MgO tunnel contacts by performing a complete characterization in applied magnetic fields up to 2.4 T, which exceeds the out-of-plane saturation field of the FM contacts. Data analysis reveals that the two-terminal magnetoresistance and the nonlocal spin signals consist of various superimposed contributions. In addition to the spin signals arising from the usual spin transport of mobile carriers through the Si channel from one FM contact to the other, there are two other contributions, namely, spin signals arising from the spin accumulation of mobile carriers in the Si channel, but generated at each of the FM contacts separately, and spin signals originating from the spin accumulation of carriers that are confined at or near the Si/MgO interface of the magnetic tunnel contacts. In the *nonlocal* spin signal, there is a clear broad Hanle signal from electrons confined at the Si/MgO interface, which is argued to be mediated by heat flow from the injector to the nonlocal detector.

II. RESULTS

The experiments were performed on lateral spin-transport devices with a 70-nm-thick *n*-type Si channel that is heavily

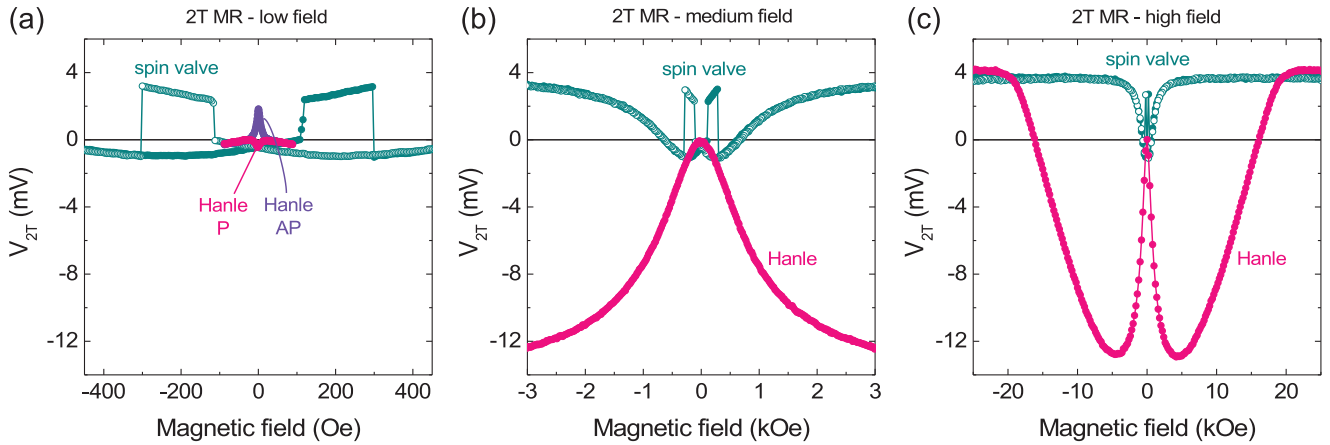


FIG. 1. Two-terminal magnetoresistance (2T MR) of a lateral spin-transport device with a Si channel and two Fe/MgO tunnel contacts at low magnetic field (a), medium field (b), and high field (c). Data is shown for the spin-valve configuration, with the external magnetic field oriented in plane, parallel to the sample surface (green data) and for the Hanle configuration, with the magnetic field perpendicular to the sample surface (pink and blue data, corresponding, respectively, to the parallel and antiparallel alignment of the magnetization of the two Fe contacts). All data was obtained at 10 K for a current of $+0.66$ mA. We subtracted the spin-independent part ($+1734$ mV) of the voltage, which arises from the Ohmic voltage drop across the Si channel plus the two tunnel contacts for a nonzero current. Note that the data in (b) and (c) were obtained using a magnetic field sweep with a larger step size (~ 20 Oe), so the narrow Hanle signals at low field are not resolved.

doped with phosphorous and patterned into a strip that is $50 \mu\text{m}$ wide and several $100 \mu\text{m}$ long. The devices have two Fe/MgO tunnel contacts, patterned by electron-beam lithography, and two additional nonmagnetic reference contacts at the ends of the Si strip. These devices have previously been used for four-terminal nonlocal and two-terminal measurements at small magnetic fields [12,23,25]. These experiments have established that a giant spin accumulation can be created in the Si channel, and that the Fe/MgO tunnel contacts exhibit a large tunnel spin polarization. Moreover, all the device parameters are known [12,13], including the value of the spin-relaxation time and the spin-diffusion length of the Si channel (18 ns and $2.4 \mu\text{m}$, respectively, at 10 K). Further details about the device fabrication and properties can be found in those previous publications [12,23,25]. Here, we have chosen one particular device for which the FM tunnel contacts have widths of 0.4 and $1.2 \mu\text{m}$, respectively, and a separation of $0.4 \mu\text{m}$. We performed nonlocal as well as two-terminal magnetoresistance (2T MR) measurements not only at small magnetic fields of the order of 10 Oe but also at higher fields of up to 24 kOe, which surpasses the out-of-plane saturation field of the Fe contacts. This provides a full characterization of the spin signals and allows us to identify the different contributions to the signals that are superimposed. All the measurements were performed at a temperature of 10 K.

A. Two-terminal magnetoresistance

In the two-terminal configuration, the two Fe/MgO contacts are used to apply the current and probe the voltage, while the nonmagnetic reference contacts are not used. The two-terminal spin signals at low magnetic field [Fig. 1(a)] exhibit familiar features. There is a clear spin-valve signal for an in-plane applied magnetic field as this switches the magnetization alignment of the two contacts between parallel (P) and antiparallel (AP). Also, for a perpendicular applied field, we observe narrow Hanle signals with a width of a few

Oe, as expected for a Si channel with a 18 ns spin-relaxation time [12], and an opposite sign of the Hanle signal for P and AP magnetization alignment. However, features that deviate from what is naively expected are also evident. First, the amplitudes of the Hanle signals for the P and AP states are significantly different. This can be understood [25] by considering a superposition of two types of spin signals, arising, respectively, from spins that are injected at one FM contact and detected by the other FM contact after transport through the Si channel and from spins that are injected into the Si channel and detected by the same FM contact. Whereas the sign of the former signal depends on the relative magnetization orientation of the two FMs, the sign of the latter signal does not, thereby creating an asymmetry between the total P and AP signal. The proper analysis of these narrow Hanle signals in the two-terminal geometry thus requires taking both contributions into account. The second feature is that the 2T spin-valve signal is evidently distorted. There is a clear curvature of the signals, the signal for the AP state has a significant slope, and the magnitude of the discontinuity in the signal at the switching field of the FM is not the same for the two FMs. It is tempting to ignore these distortions, attributing them to a nonideal switching of the magnetization. However, inspection of the shape of the spin signal in the nonlocal measurement geometry in the exact same device [to be presented below in Fig. 2(a)] already indicates that this is not correct.

When the 2T signal is studied at higher magnetic field, it becomes evident that the distortion of the spin-valve signal is nontrivial and due to an additional genuine spin signal. For medium fields [Fig. 1(b)], a distinctly different Hanle signal with a half width of the order of 1 kOe is visible, and for in-plane fields a similarly broad signal with the opposite sign is observed. At even higher fields [Fig. 1(c)], the in-plane signal saturates at a constant level, whereas the Hanle signal has a minimum around 4–5 kOe, after which the signal increases due to the out-of-plane rotation of the Fe contacts in the large perpendicular magnetic field. The Hanle signal saturates

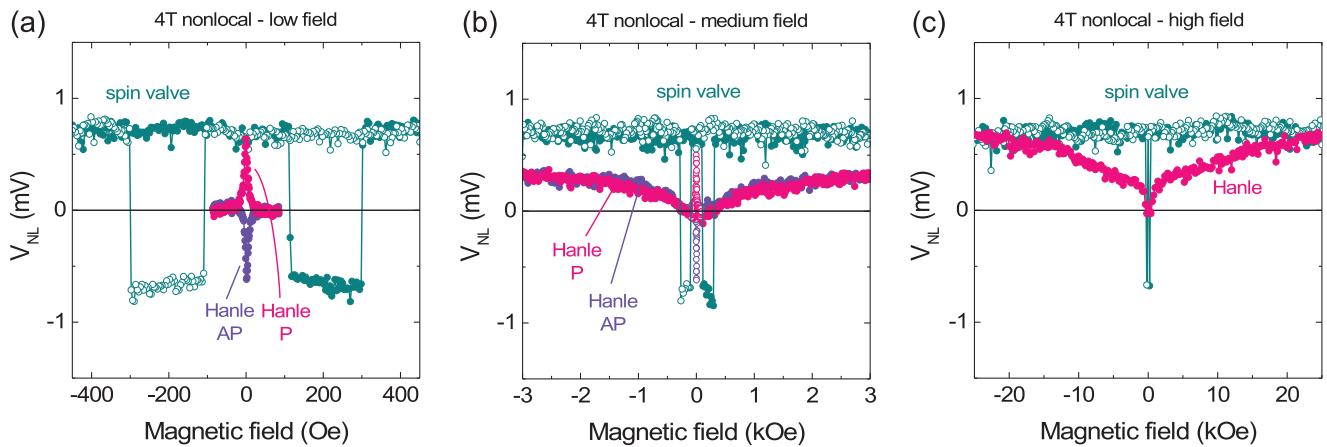


FIG. 2. Four-terminal nonlocal spin signals of a silicon device with Fe/MgO tunnel contacts at low magnetic field (a), medium field (b), and high field (c). Data is shown for the spin-valve configuration, with the external magnetic field oriented in plane, parallel to the sample surface (green data) and for the Hanle configuration, with the magnetic field perpendicular to the sample surface (pink and blue data, corresponding, respectively, to the parallel and antiparallel alignment of the magnetization of the two Fe contacts). All data was obtained at 10 K for a current of +0.66 mA. A nonlocal offset voltage of +3.25 mV was subtracted. In panel (b), we added the high-resolution Hanle data for the P and the AP configuration taken at low fields [pink and blue open symbols, respectively]. This is the same data as in panel (a).

above 20 kOe, at which the Fe magnetization is fully out of plane. These broad Hanle signals, which have been widely observed in *three*-terminal measurements on single magnetic tunnel contacts on semiconductors [31–40], are genuine Hanle [32] and inverted Hanle [33] signals due to the spin precession of a spin accumulation (nonequilibrium spin density), albeit from spins that are not diffusing in the Si channel. Rather, the broad signals are thought [31,41] to be produced by spins that are confined at or near the Si/MgO interface or in the Si depletion region [40], although the precise nature and location of these confined spins has yet to be clarified [39,40]. We do not aim to resolve this here. The important message here is that the broad Hanle and inverted Hanle signals, which are produced separately for both of the two FM tunnel contacts by the nonzero current, are a genuine part of the 2T magnetoresistance signal of a lateral spin-transport device [42]. Moreover, the broad Hanle signal is much larger than the signal produced by the mobile electrons in the Si channel.

B. Nonlocal spin signals

Next, we examine the nonlocal spin signals measured in the exact same device, applying the current between one of the Fe/MgO contacts and the adjacent nonmagnetic reference contact, while the nonlocal voltage is measured between the second Fe/MgO contact and the other nonmagnetic contact. At low fields [Fig. 2(a)], a clear spin-valve signal is observed for in-plane applied magnetic field. The observed narrow Hanle signals for a perpendicular applied field have the opposite sign for the P and the AP configuration and also have an equal amplitude that matches with the spin-valve signal. These results are as expected for spin signals generated by mobile electrons diffusing through the Si from the injector to the detector contact. However, this is not the only contribution to the nonlocal spin signal, which becomes clear when measurements at larger magnetic fields are performed. At medium magnetic fields [Fig. 2(b)], it is found that an additional signal is present, since the Hanle signals clearly deviate from zero

for fields above a few hundred Oe. This is not expected, because for such fields the spin accumulation in the Si channel is fully suppressed by spin precession in the perpendicular field, while magnetic fields of the order of a kOe do not cause any significant rotation of the contact magnetization into the out-of-plane direction (as shown below in the analysis section). For larger perpendicular magnetic fields up to 20 kOe [Fig. 2(c)], the Hanle signal gradually increases because of the out-of-plane rotation of the Fe magnetization, which reduces the angle between the field and the spins. Consequently, the spin accumulation fully recovers above 20 kOe and the signal for in-plane and perpendicular field becomes the same, since in both cases there is no spin precession. Most importantly, however, a clear dip in the Hanle signal can be seen for fields of a few kOe, and, in fact, the width of this additional signal is of the order of a 1 kOe and thus similar to that of the broad Hanle signal observed in the 2T MR [Fig. 1(b)]. This suggests that a broad Hanle spin signal is not only present in the 2T MR but also in the nonlocal spin signal (see below for a more detailed analysis). Importantly, for fields above a hundred Oe, the nonlocal Hanle signals for the P and the AP configuration are identical, implying that the additional (broad) nonlocal Hanle signal does not depend on whether the magnetizations of the injector and the detector are P or AP.

III. ANALYSIS OF THE SPIN SIGNALS

The detailed description of the low-field spin signals due to the spin accumulation and diffusion in the Si channel was presented in our previous publications [12,23,25]. Therefore, we focus our analysis here on the superimposed spin signals that dominate the medium- and high-field range, starting with the two-terminal MR.

A. Analysis of the two-terminal magnetoresistance

The 2T MR at medium and high fields is dominated by the broad Hanle and inverted Hanle signals. These are described

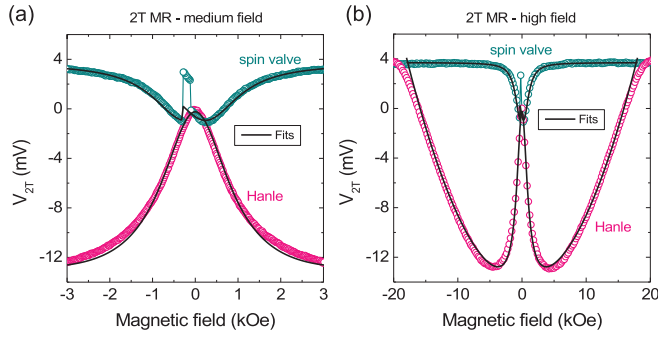


FIG. 3. Two-terminal magnetoresistance data (symbols) together with fits (solid lines) of the broad Hanle and inverted Hanle signals produced by electrons confined at the MgO/Si interfaces of the magnetic tunnel contacts. Experimental data obtained at 10 K for a current of +0.66 mA is shown for medium (a) and high magnetic field (b) for the spin-valve configuration (green symbols) and for the Hanle configuration (pink symbols). For the spin-valve data, only one trace (field sweep from + to -) is shown.

[33] by the following equation for the spin precession of a confined spin accumulation without spin diffusion:

$$S = S_0 \left\{ \frac{\omega_y^2}{\omega_L^2} + \left(\frac{\omega_x^2 + \omega_z^2}{\omega_L^2} \right) \cdot \left(\frac{1}{1 + (\omega_L \tau_s^i)^2} \right) \right\}, \quad (1)$$

with S the spin density projected onto the magnetization direction of the magnetic contact and S_0 the spin density in the absence of any magnetic fields. The effective spin-relaxation time τ_s^i corresponds to confined electrons at the MgO/Si interface. The Larmor frequency ω_L has components $(\omega_x, \omega_y, \omega_z) = (g\mu_B/\hbar)(B_x, B_y, B_z)$, where g is the Landé n factor, μ_B is the Bohr magneton, \hbar is Planck's constant divided by 2π . The components B_i of the magnetic field include not only the external applied magnetic field but also any internal fields. We included the internal magnetostatic field that is produced near a FM interface with finite roughness and which causes the inverted Hanle effect [33]. To mimic this, we included a constant magnetostatic field (B^{ms}) in the x direction, which is in plane but orthogonal to the long axis of the FM contact strips (y direction). Second, we take into account the exchange field (B^{exch}) that the FM contact exerts on the precessing spins near the MgO/Si interface [43]. It is taken to be constant and locked P to the magnetization direction of the Fe contact [43,44]. For a perpendicular external field B_z , the out-of-plane rotation of the magnetization was accounted for by rotating the coordinate system in the $y-z$ plane by an angle θ , which is defined via $\cos(\theta) = B_z/B_{\text{sat}}$, with $B_{\text{sat}} = 18$ kOe the out-of-plane saturation field of the Fe contact. This assumes a simple linear increase of the z component of the magnetization with increasing B_z .

By choosing $B^{\text{ms}} = 465$ Oe, $B^{\text{exch}} = 240$ Oe, $\tau_s^i = 72$ ps, and adjusting the overall prefactor, we obtain a rather good description of the two-terminal MR data at medium and high field (Fig. 3). The slight differences between the fit and the Hanle data are attributed to the idealized description of the out-of-plane rotation of the Fe magnetization. The fit for the in-plane field reveals that the inverted Hanle effect creates curvature of the signal in the low-field region, a nonzero slope in

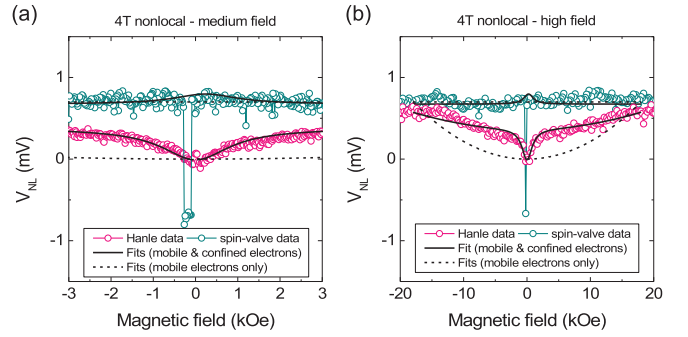


FIG. 4. Nonlocal spin signals (symbols) together with fits (solid and dashed lines) at medium (a) and high magnetic field (b). For the dashed lines, only the contribution of mobile electrons in the Si channel was considered. For the solid lines, also a contribution from electrons confined at the MgO/Si interfaces of the magnetic tunnel contacts was included, using the same parameters as for the fit of the 2T MR data in Fig. 3, except for the prefactor, which is adjusted to match the overall magnitude. Experimental data obtained at 10 K for a current of +0.66 mA is shown for the spin-valve configuration (green symbols) and for the Hanle configuration (pink symbols). For the spin-valve data, only one trace (field sweep from + to -) is shown.

the AP state, and a discontinuity at the coercive field of the Fe electrode (caused by the exchange field [43,44]). These features explain the distortions of the low-field spin-valve signal that we described in Sec. II A. Note, however, that the fit for the in-plane field deviates from the experimental data in the region where the Fe contacts have AP magnetization (between -110 and -300 Oe) because the fits do not include the delocalized electrons in the Si channel, whose contribution causes the signal to be different for the P and the AP magnetization alignment. Adding the latter contribution would reproduce all the features of the spin signals. We conclude that the 2T MR is described well by a contribution from delocalized electrons in the Si channel and a superimposed contribution from the confined electrons at the MgO/Si interfaces of the tunnel contacts.

B. Analysis of the nonlocal spin signals

For the description of the nonlocal spin signals, we start with the common assumption that the nonlocal signal is exclusively determined by mobile electron spins in the Si channel that are transported from the injector to the detector contact. The associated spin signal for medium and high magnetic fields is expected to vary, as indicated by the dashed lines in Fig. 4. To obtain these fits, we first used the data at very small magnetic fields [depicted in Fig. 2(a)] to fit the narrow Hanle peaks, using the previously determined values [12,13] of the spin-relaxation time τ_s (18 ns) and the spin-diffusion length ($2.4 \mu\text{m}$). Next, we included the gradual out-of-plane rotation of the magnetization of the Fe contacts in a perpendicular field using Eq. (1), but replacing τ_s^i by the spin-relaxation time of mobile electrons in the Si channel (18 ns). Also, we omitted the internal fields B^{ms} and B^{exch} that were introduced to describe the broad Hanle and inverted Hanle signals of the confined electrons because the observed narrow nonlocal

Hanle signals at small fields [Fig. 2(a)] cannot be described if there is any significant magnetostatic stray field or exchange field acting on the mobile spins in the Si channel [45]. Whereas the narrow nonlocal Hanle peaks at small fields are well described by considering only the mobile electron in the Si channel [12,13], the dashed line fits in Fig. 4 show that the nonlocal spin signals at medium and high fields cannot be reproduced. In particular, the nonlocal Hanle signal is predicted to remain close to zero for perpendicular fields up to a few kOe [Fig. 4(a)] because a significant out-of-plane rotation does not occur in this field range (for instance, for $B_z = 2$ kOe, $\cos(\theta) = 0.11$, corresponding to an out-of plane rotation of 6° only). This clearly demonstrates that by considering only the mobile spins in the Si channel, the nonlocal Hanle signal in the few kOe range cannot be described. Hence, an additional contribution is needed to describe the nonlocal Hanle signals.

Since the width of the additional nonlocal Hanle signal is of the order of a few kOe and similar to the broad Hanle signals observed in the two-terminal (and three-terminal) geometry, we include a broad Hanle signal due to confined electrons at the MgO/Si interface, as described by Eq. (1). The parameters τ_s^i , B^{ms} , and B^{exch} are the same as those used to fit the 2T MR, whereas the prefactor, which controls the overall amplitude of the signal, was adjusted to match the nonlocal Hanle signal in the few kOe range. Adding this to the signal from the mobile electrons results in the solid line fits in Fig. 4. These fits provide an adequate description of the nonlocal spin signal in the medium and high-field range. This demonstrates that the nonlocal spin signal has a clear contribution from spins that are confined near the MgO/Si interfaces, rather than being determined exclusively by mobile electrons in the Si channel, as was hitherto thought.

C. Origin of the broad nonlocal Hanle signal

Let us discuss the possible origin of the observed broad Hanle contribution to the nonlocal spin signal. Since it does not depend on the relative alignment of the magnetization of the two FM contacts (P or AP), it does not originate from electron spins that are transported from one contact to the other. However, it is known from three-terminal measurements that a broad Hanle signal can be produced by a single magnetic tunnel contact under a current bias [32,33]. Nevertheless, in a nonlocal measurement there is no charge current across the detector contact and hence there is no electrically generated broad Hanle signal in the detector [46]. Therefore, we considered the possibility that a broad Hanle signal that is generated in the (biased) injector Fe/MgO/Si junction is imprinted in the nonlocal detector voltage due to a finite coupling between the injector and the nonlocal detector. Such a coupling should be absent in an ideal nonlocal device but, in practice, the nonlocal measurement is never perfectly ideal. The coupling, which is electric [47] and/or thermoelectric [48–51] in nature, is consistently observed and is known to cause a nonzero offset in the nonlocal detector voltage. The finite coupling in a nonideal nonlocal device may allow (a fraction of the) signals that are generated in the injector contact itself to appear in the nonlocal output signal.

It is tempting to estimate what the expected broad nonlocal Hanle signal is by assuming that the ratio of the broad Hanle

signal and the charge voltage across the contact is the same for the detector and the injector. From a standard three-terminal measurement geometry, the voltage across the injector tunnel contact was determined to be $+1140$ mV ($+1131.6$ mV) at $B = 0$ ($B = \pm 4$ kOe) for a current of $+0.66$ mA, which yields a broad Hanle signal of $+8.4$ mV, with a positive sign. In the nonlocal measurement, an offset of $+3.25$ mV was observed for the same current [52]. One then would expect a broad Hanle signal of $(+3.25/+1140) \times +8.4$ mV = $+0.024$ mV in the detected nonlocal voltage. The observed broad Hanle contribution to the nonlocal signal is -0.36 mV. This is much larger than the expected signal (by a factor of 15), and, perhaps more importantly, the observed signal has the *opposite* sign. However, as we will see below, this simple estimate is way too oversimplified. We therefore discuss the coupling mechanisms in more detail.

Let us first discuss purely electric injector-detector coupling [47]. It is determined by deviations from a perfectly uniform charge current and potential distribution in the channel, which depends on the precise geometry and dimensions of the channel and the magnetic contacts and on any other factors that might introduce nonuniformity. Such nonuniformities lead to a nonzero charge current density in the part of the channel that is located on the detector side of the injector, thereby causing a finite offset in the detected nonlocal voltage. As shown in the Appendix, for the device geometry and the wiring arrangement that we used, the electric coupling should produce a nonlocal offset with a positive sign, as is observed. Since the broad Hanle signal of the injector junction is also positive, one would *not* expect a broad nonlocal Hanle signal with a negative sign (-0.36 mV) to appear at the nonlocal detector. In fact, we argue that a purely electric coupling should not imprint any Hanle spin signal in the nonlocal detector voltage, because the measurement is performed with a *constant current* across the injector contact. Consequently, when a magnetic field is applied and the spin accumulation at the interface of the injector tunnel contact changes, the voltage across the injector tunnel contact changes but the current distribution in the channel does not [53]. Since for purely electric injector-detector coupling the nonlocal offset is proportional to the *current* and its nonuniform distribution in the channel [47], the offset is not affected by the applied magnetic field. Hence, the observed broad nonlocal Hanle signal is not due to electric coupling between injector and detector.

The other source of injector-detector coupling is thermoelectric in nature. It produces an offset voltage in the nonlocal detector circuit in the following way. The injected current causes Joule heating in the entire current path as well as Peltier heating/cooling at the injector junction [48,49]. Transport of the heat creates a temperature gradient along the channel as well as heat flow across the detector junction, which, via the Seebeck effect, are converted back into a charge voltage across the detector junction [Fig. 5(a)]. It is very well possible that this thermoelectric coupling produces an offset of the nonlocal voltage [48,49]. However, the pertinent question here is whether this mechanism can also produce the detected broad nonlocal Hanle signal. More precisely, the question is whether the heating/cooling and the resulting heat flows in the device are changed when a magnetic field induces spin precession of the confined electrons at the injector MgO/Si

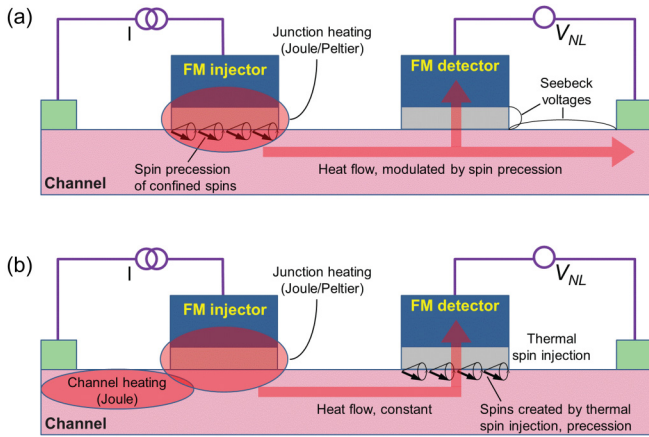


FIG. 5. Schematic illustration of the mechanisms that can produce a broad Hanle signal from interface-confined electrons in a nonlocal measurement. (a) Joule or Peltier heating in the ferromagnetic injector contact, which is modulated by the spin precession of the confined electron spins near the injector interface. The resulting magnetic field-dependent heat flow through the device is converted into a magnetic field-dependent charge voltage in the nonlocal detector circuit via the Seebeck effect. (b) Heat generated by the injection current causes a heat flow across the detector Si/MgO/Fe junction, which, via thermal spin injection by Seebeck spin tunneling, creates a spin accumulation of confined electrons near the detector interface. These confined electron spins, in turn, produce a broad nonlocal Hanle signal

interface. Joule heating in the Si channel does not change because the current is kept constant. However, the broad Hanle effect changes the voltage across the injector tunnel contact and thereby the Joule heating produced by the injector tunnel contact (which is proportional to the product of the tunnel current and the tunnel voltage). This, in turn, will change the magnitude of the heat flows in the device [Fig. 5(a)], and thereby the nonlocal offset voltage, imprinting a broad injector Hanle signal in the nonlocal detector voltage. Furthermore, we argue that a spin signal may also be imprinted via Peltier heating/cooling because it is proportional to the current (constant) and the Peltier coefficient of the tunnel contact, and the latter is expected to depend on spin [54,55]. Consequently, a change in the spin accumulation of electrons confined at the injector MgO/Si interface will result in a change of the effective Peltier coefficient of the injector tunnel contact, and thereby change the heat flows in the device [Fig. 5(a)]. Hence, we argue that Joule heating as well as Peltier heating/cooling are affected by the spin precession of confined electrons at the injector interface and that because the nonlocal offset voltage is proportional to the heat flow in the device, this allows the broad Hanle signal to be imprinted in the nonlocal detector signal. This can be viewed as magnetic control of heat flow.

There is a third mechanism that we have not yet considered [Fig. 5(b)]. Even in the absence of a charge current across the detector junction, a spin accumulation of electrons confined at the detector MgO/Si interface can still be generated by the heat flow across the detector tunnel contact via an effect known as Seebeck spin tunneling [56]. It originates from the spin dependence of the Seebeck coefficient of a magnetic

tunnel contact [56]. This causes a temperature gradient across the detector tunnel contact to induce a spin current and a spin accumulation of the confined electrons at the MgO/Si interface, with the associated broad Hanle signal. Although this mechanism is also determined by the heat flows in the device, the relevant spins are located at the detector interface [Fig. 5(b)]. In contrast, for the two mechanisms described in the previous paragraph, the relevant spins are confined at the injector interface [Fig. 5(a)]. The first mechanism (imprinting via Joule heating) does not rely on the spin dependence of the Peltier and Seebeck coefficient of the magnetic tunnel contacts, whereas the other two mechanisms do.

IV. DISCUSSION

We have shown that the 2T-MR signal has three contributions: (i) spin signals arising from spin transport of mobile carriers through the Si channel from one FM contact to the other, (ii) spin signals arising from the spin accumulation of mobile carriers in the Si channel but generated at each of the FM contacts separately, and (iii) spin signals originating from spin accumulation of carriers that are confined at or near the Si/MgO interface of the magnetic tunnel contacts. The local contributions (ii) and (iii) can be separated out by performing suitable three-terminal measurements, in which the contribution from the transport of mobile carriers through the channel is eliminated, as previously demonstrated [23,25].

For the nonlocal signal, only two contributions were identified [(i) and (iii)]. It is relatively easy to distinguish between these two different signals for *n*-type silicon because the spin-relaxation time of mobile electrons is of the order of 10 ns at low temperature, and so the width of the corresponding Hanle signal is small and very different from that of the broad Hanle signals that are attributed to electrons confined at the Si/MgO interface. However, for other material systems, the widths of the two types of Hanle signals may be more comparable, in which case disentangling the different signal contributions is not as straightforward. Moreover, although we have not identified the presence of contribution (ii) in the nonlocal spin signal, in general, this contribution should be considered as well. It is known that the Hanle signal generated by a single tunnel contact, such as measured in a three-terminal configuration, has a contribution from mobile carriers in the channel. For devices with a Si channel this produces a narrow Hanle signal in the voltage across the magnetic tunnel contact [57], in addition to the broad Hanle signal due to confined electrons at the MgO/Si interface. The same thermal mechanisms that imprint the broad Hanle signal from the injector contact onto the nonlocal detector will also imprint the narrow Hanle signal from the injector contact onto the nonlocal detector signal. And since this imprinted narrow nonlocal signal would not depend on whether the magnetization alignment is P or AP, the measured nonlocal Hanle signals for P and AP states will have an unequal amplitude, while the width of the nonlocal Hanle signals may also be affected.

As for the origin of the broad nonlocal Hanle signal, although it is argued to be of a thermal origin, the precise mechanism has yet to be established. It might be possible to determine the thermal source (Joule heating or Peltier heating/cooling) because of their different dependence on the

current (quadratic versus linear, respectively). However, some of the parameters, such as the tunnel spin polarization of the Fe/MgO tunnel contacts, will not be constant as a function of the current. It is more complicated to establish whether the signal comes from confined electrons at the injector or the detector contact, because in both cases the same heat flow mediates the effect. We envision that a special set of devices with one FM contact and one non-FM contact can shed light on this.

V. SUMMARY

The spin voltages produced by spin accumulation and Hanle spin precession in a spin-transport device composed of a lateral silicon channel and FM tunnel contacts (Fe/MgO) were probed at low magnetic fields and at high fields exceeding the out-of-plane anisotropy field of the Fe contacts. Analysis of the two-terminal magnetoresistance as well as the nonlocal spin signals reveals that these signals are a superposition of (i) spin signals arising from spin transport of mobile carriers through the Si channel from one FM contact to the other, thus depending on the relative magnetization of the two contacts, (ii) spin signals also arising from the spin accumulation of mobile carriers in the Si channel but generated at each of the FM contacts separately, and (iii) spin signals originating from spin accumulation of carriers that are confined at or near the Si/MgO interface of the magnetic tunnel contacts, with rather different spin precession characteristics. The surprising observation of a broad Hanle signal from confined electrons in the *nonlocal* measurement geometry is attributed to a thermal effect. The analysis of the spin signals in such devices thus requires careful characterization and disentanglement of the different superimposed contributions.

ACKNOWLEDGMENT

We acknowledge financial support by the Grant-in-Aid for Scientific Research on Innovative Areas, Nano Spin Conversion Science (Grants No. 26103002 and No. 26103003).

APPENDIX

In this Appendix we discuss the expected sign of the offset voltage that is produced by the electric nonuniformity of our nonlocal transport device (Fig. 6). The resistance of the FM tunnel contacts is much larger than the sheet resistance of the channel. Therefore, the charge current that is injected into the channel is uniformly distributed over the area of the injector contact. Second, the channel thickness (70 nm) is much smaller than the width or the spacing of the FM contacts, so nonuniformity in the perpendicular direction does not play any significant role either [47]. The nonuniformity in our device is mainly caused by the fact [58] that the length $L_y = 40 \mu\text{m}$ of the FM contacts along the y direction is smaller than the width $W_y = 50 \mu\text{m}$ of the Si channel [Fig. 6(a)]. This causes a nonuniform lateral distribution of the charge current in the channel.

To determine the sign of the offset voltage this produces, we first consider the ideal case, for which the length of the FM contacts is equal to the channel width [Fig. 6(b), depicting

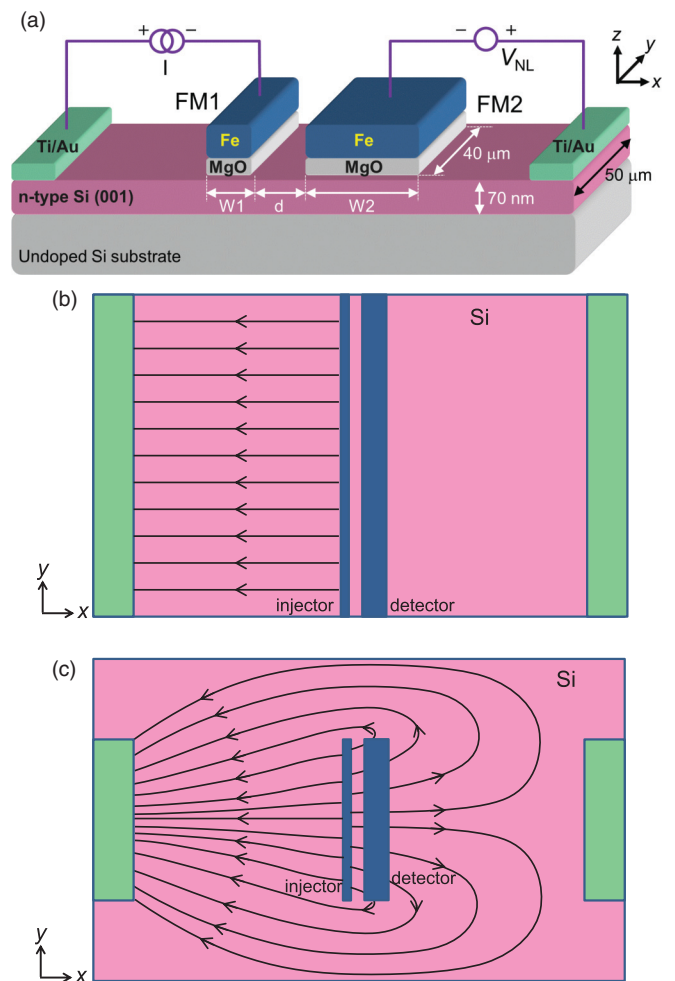


FIG. 6. (a) Layout of the spin-transport device and the nonlocal measurement configuration, with the lateral dimensions of the channel and the ferromagnetic contacts indicated. Panels (b) and (c) depict a schematic view of the distribution of the *charge* flow in an ideal device (b) and in a device in which the length of the ferromagnetic contacts is smaller than the width of the channel (c). The current in the injector circuit is assumed to be positive, corresponding to the injection of electrons from the ferromagnet into the Si channel. The arrows indicate the direction of the *electron* flow.

the electron flow distribution for a positive injector current, corresponding to the injection of electrons into the channel]. In the ideal case, the charge current is uniform on the left side of the injector contact, and the charge current density vanishes everywhere to the right of the injector. Hence, no nonlocal offset voltage is produced. Figure 6(c) shows the electron flow distribution when the length of the FM injector contact is significantly smaller than the channel width. In this case, the charge current density is nonzero on the right side of the injector, with electrons flowing toward the right near the center of the channel and returning back to the left near the edges of the channel. Now, because the length of the detector contact is also smaller than the width of the channel, the detector will mainly probe the potential near the center of the device, where electrons are flowing to the right. This will produce a nonzero nonlocal offset voltage with a positive sign for the wiring configuration depicted in Fig. 6(a). Hence,

electrical nonuniformity should produce a positive nonlocal offset voltage for a positive injector voltage/current. Because only a small part of the charge current goes toward the right, the offset voltage is a small fraction of the applied injector

voltage. The magnitude of the offset voltage is linearly proportional to the injected charge current and to the sheet resistance of the Si channel [47] and, in our specific case, depends on the ratio of L_y and W_y .

- [1] I. Žutić, J. Fabian, and S. Das Sarma, Spintronics: Fundamentals and applications, *Rev. Mod. Phys.* **76**, 323 (2004).
- [2] A. Fert, Nobel lecture: Origin, development, and future of spintronics, *Rev. Mod. Phys.* **80**, 1517 (2008).
- [3] S. Sugahara and J. Nitta, Spin-transistor electronics: An overview and outlook, *Proc. IEEE* **98**, 2124 (2010).
- [4] R. Jansen, Silicon spintronics, *Nature Mater.* **11**, 400 (2012).
- [5] M. Johnson and R. H. Silsbee, Interfacial Charge-Spin Coupling: Injection and Detection of Spin Magnetization in Metals, *Phys. Rev. Lett.* **55**, 1790 (1985).
- [6] F. J. Jedema, H. B. Heersche, A. T. Filip, J. J. A. Baselmans, and B. J. van Wees, Electrical detection of spin precession in a metallic mesoscopic spin valve, *Nature* **416**, 713 (2002).
- [7] T. Kimura, J. Hamrle, Y. Otani, K. Tsukagoshi, and Y. Aoyagi, Suppression of spin accumulation in nonmagnet due to ferromagnetic ohmic contact, *Appl. Phys. Lett.* **85**, 3795 (2004).
- [8] S. O. Valenzuela, D. J. Monsma, C. M. Marcus, V. Narayanamurti, and M. Tinkham, Spin Polarized Tunneling at Finite Bias, *Phys. Rev. Lett.* **94**, 196601 (2005).
- [9] N. Tombros, C. Jozsa, M. Popinciuc, H. T. Jonkman, and B. J. van Wees, Electronic spin transport and spin precession in single graphene layers at room temperature, *Nature* **448**, 571 (2007).
- [10] X. Lou, C. Adelman, S. A. Crooker, E. S. Garlid, J. Zhang, K. S. M. Reddy, S. D. Flexner, C. J. Palmstrøm, and P. A. Crowell, Electrical detection of spin transport in lateral ferromagnet-semiconductor devices, *Nat. Phys.* **3**, 197 (2007).
- [11] M. Yamada, M. Tsukahara, Y. Fujita, T. Naito, S. Yamada, K. Sawano, and K. Hamaya, Room-temperature spin transport in n-Ge probed by four-terminal nonlocal measurements, *Appl. Phys. Express* **10**, 093001 (2017).
- [12] A. Spiesser, H. Saito, Y. Fujita, S. Yamada, K. Hamaya, S. Yuasa, and R. Jansen, Giant Spin Accumulation in Silicon Nonlocal Spin-Transport Devices, *Phys. Rev. Appl.* **8**, 064023 (2017).
- [13] A. Spiesser, H. Saito, S. Yuasa, and R. Jansen, Tunnel spin polarization of Fe/MgO/Si contacts reaching 90% with increasing MgO thickness, *Phys. Rev. B* **99**, 224427 (2019).
- [14] T. Sasaki, T. Oikawa, T. Suzuki, M. Shiraishi, Y. Suzuki, and K. Noguchi, Local and non-local magnetoresistance with spin precession in highly doped Si, *Appl. Phys. Lett.* **98**, 262503 (2011).
- [15] P. Bruski, Y. Manzke, R. Farshchi, O. Brandt, J. Herfort, and M. Ramsteiner, All-electrical spin injection and detection in the $\text{Co}_2\text{FeSi}/\text{GaAs}$ hybrid system in the local and non-local configuration, *Appl. Phys. Lett.* **103**, 052406 (2013).
- [16] T. Sasaki, T. Suzuki, Y. Ando, H. Koike, T. Oikawa, Y. Suzuki, and M. Shiraishi, Local magnetoresistance in Fe/MgO/Si lateral spin valve at room temperature, *Appl. Phys. Lett.* **104**, 052404 (2014).
- [17] Y. Saito, T. Tanamoto, M. Ishikawa, H. Sugiyama, T. Inokuchi, K. Hamaya, and N. Tezuka, Effects of interface electric field on the magnetoresistance in spin devices, *J. Appl. Phys.* **115**, 17C514 (2014).
- [18] T. Tahara, H. Koike, M. Kameno, T. Sasaki, Y. Ando, K. Tanaka, S. Miwa, Y. Suzuki, and M. Shiraishi, Room-temperature operation of Si spin MOSFET with high on/off spin signal ratio, *Appl. Phys. Express* **8**, 113004 (2015).
- [19] D. D. Hiep, M. Tanaka, and P. N. Hai, Spin transport in nanoscale Si-based spin-valve devices, *Appl. Phys. Lett.* **109**, 232402 (2016).
- [20] M. Gurram, S. Omar, and B. J. van Wees, Bias induced up to 100% spin-injection and detection polarizations in ferromagnet/bilayer-hBN/graphene/hBN heterostructures, *Nat. Commun.* **8**, 248 (2017).
- [21] M. Oltscher, F. Eberle, T. Kuczmik, A. Bayer, D. Schuh, D. Bougeard, M. Ciorga, and D. Weiss, Gate-tunable large magnetoresistance in an all-semiconductor spin valve device, *Nat. Commun.* **8**, 1807 (2017).
- [22] M. Ishikawa, M. Tsukahara, M. Yamada, Y. Saito, and K. Hamaya, Local magnetoresistance at room temperature in Si(100) devices, *IEEE Trans. Mag.* **54**, 1400604 (2018).
- [23] R. Jansen, A. Spiesser, H. Saito, Y. Fujita, S. Yamada, K. Hamaya, and S. Yuasa, Nonlinear Electrical Spin Conversion in a Biased Ferromagnetic Tunnel Contact, *Phys. Rev. Appl.* **10**, 064050 (2018).
- [24] M. Tsukahara, M. Yamada, T. Naito, S. Yamada, K. Sawano, V. K. Lazarov, and K. Hamaya, Room-temperature local magnetoresistance effect in n-Ge devices with low-resistive Schottky-tunnel contacts, *Appl. Phys. Express* **12**, 033002 (2019).
- [25] A. Spiesser, Y. Fujita, H. Saito, S. Yamada, K. Hamaya, S. Yuasa, and R. Jansen, Hanle spin precession in a two-terminal lateral spin valve, *Appl. Phys. Lett.* **114**, 242401 (2019).
- [26] K. Kudo, M. Yamada, S. Honda, Y. Wagatsuma, S. Yamada, K. Sawano, and K. Hamaya, Room-temperature two-terminal magnetoresistance ratio reaching 0.1% in semiconductor-based lateral devices with L_{21} -ordered Co_2MnSi , *Appl. Phys. Lett.* **118**, 162404 (2021).
- [27] Z. G. Yu and M. E. Flatté, Spin diffusion and injection in semiconductor structures: Electric field effects, *Phys. Rev. B* **66**, 235302 (2002).
- [28] C. Jozsa, M. Popinciuc, N. Tombros, H. T. Jonkman, and B. J. van Wees, Electronic Spin Drift in Graphene Field-Effect Transistors, *Phys. Rev. Lett.* **100**, 236603 (2008).
- [29] T. Sasaki, Y. Ando, M. Kameno, T. Tahara, H. Koike, T. Oikawa, T. Suzuki, and M. Shiraishi, Spin Transport in Nondegenerate Si with a Spin MOSFET Structure at Room Temperature, *Phys. Rev. Appl.* **2**, 034005 (2014); **9**, 039901(E) (2018).
- [30] A. Spiesser, Y. Fujita, H. Saito, S. Yamada, K. Hamaya, W. Mizubayashi, K. Endo, S. Yuasa, and R. Jansen, Quantification of Spin Drift in Devices with a Heavily Doped Si Channel, *Phys. Rev. Appl.* **11**, 044020 (2019).

- [31] M. Tran, H. Jaffrès, C. Deranlot, J.-M. George, A. Fert, A. Miard, and A. Lemaître, Enhancement of the Spin Accumulation at the Interface Between a Spin-Polarized Tunnel Junction and a Semiconductor, *Phys. Rev. Lett.* **102**, 036601 (2009).
- [32] S. P. Dash, S. Sharma, R. S. Patel, M. P. de Jong, and R. Jansen, Electrical creation of spin polarization in silicon at room temperature, *Nature* **462**, 491 (2009).
- [33] S. P. Dash, S. Sharma, J. C. Le Breton, J. Peiro, H. Jaffrès, J.-M. George, A. Lemaître, and R. Jansen, Spin precession and inverted Hanle effect in a semiconductor near a finite-roughness ferromagnetic interface, *Phys. Rev. B* **84**, 054410 (2011).
- [34] K. R. Jeon, B. C. Min, Y. H. Jo, H. S. Lee, I. J. Shin, C. Y. Park, S. Y. Park, and S. Ch. Shin, Electrical spin injection and accumulation in CoFe/MgO/Ge contacts at room temperature, *Phys. Rev. B* **84**, 165315 (2011).
- [35] M. Ishikawa, H. Sugiyama, T. Inokuchi, K. Hamaya, and Y. Saito, Effect of the interface resistance of CoFe/MgO contacts on spin accumulation in silicon, *Appl. Phys. Lett.* **100**, 252404 (2012).
- [36] A. Jain, C. Vergnaud, J. Peiro, J. C. Le Breton, E. Prestat, L. Louahadj, C. Portemont, C. Ducruet, V. Baltz, A. Marty, A. Barski, P. Bayle-Guillemaud, L. Vila, J.-P. Attané, E. Augendre, H. Jaffrès, J.-M. George, and M. Jamet, Electrical and thermal spin accumulation in germanium, *Appl. Phys. Lett.* **101**, 022402 (2012).
- [37] R. Jansen, S. P. Dash, S. Sharma, and B. C. Min, Silicon spintronics with ferromagnetic tunnel devices, *Semicond. Sci. Technol.* **27**, 083001 (2012).
- [38] T. Uemura, K. Kondo, J. Fujisawa, K. Matsuda, and M. Yamamoto, Critical effect of spin-dependent transport in a tunnel barrier on enhanced Hanle-type signals observed in three-terminal geometry, *Appl. Phys. Lett.* **101**, 132411 (2012).
- [39] S. Sharma, A. Spiesser, S. P. Dash, S. Iba, S. Watanabe, B. J. van Wees, H. Saito, S. Yuasa, and R. Jansen, Anomalous scaling of spin accumulation in ferromagnetic tunnel devices with silicon and germanium, *Phys. Rev. B* **89**, 075301 (2014).
- [40] A. Spiesser, H. Saito, R. Jansen, S. Yuasa, and K. Ando, Large spin accumulation voltages in epitaxial Mn₅Ge₃ contacts on Ge without an oxide tunnel barrier, *Phys. Rev. B* **90**, 205213 (2014).
- [41] Y. Song and H. Dery, Magnetic-Field-Modulated Resonant Tunneling in Ferromagnetic-Insulator-Nonmagnetic Junctions, *Phys. Rev. Lett.* **113**, 047205 (2014).
- [42] The 2T MR also has a contribution from the regular magnetoresistance of the Si channel. However, the resistance of the channel is only a small fraction ($\sim 6 \Omega$) of the total 2T resistance (2627 Ω), which is dominated by the tunnel contacts in our device. Therefore, the contribution of the Si channel to the 2T MR is negligibly small ($< 40 \mu\text{V}$ for the current of 0.66 mA used, whereas the spin-valve signal is about 4 mV).
- [43] R. Jansen, A. Spiesser, H. Saito, Y. Fujita, S. Yamada, K. Hamaya, and S. Yuasa, Proximity exchange coupling in a Fe/MgO/Si tunnel contact detected by the inverted Hanle effect, *Phys. Rev. B* **100**, 174432 (2019).
- [44] The discontinuity in the inverted Hanle curve arises in the following way [43]. The exchange field, which is collinear with the external in-plane field, shifts the minimum of the inverted Hanle curve away from zero field. Because the exchange field is locked parallel to the magnetization of the Fe contact, the exchange field changes signs when the Fe magnetization is reversed at the coercive field. As a result, the direction of the shift is also reversed, producing a discontinuity in the signal at the coercive field.
- [45] Even a small internal field (exchange or magnetostatic stray field) acting on the mobile spins in the Si channel would cause a significant broadening of the nonlocal Hanle signals to a width that is well beyond the few Oe set by the 18 ns spin-relaxation time. Also, any internal field components orthogonal to the spins would produce a nonlocal inverted Hanle signal (not observed) and a reduction of the amplitude of the Hanle peaks (which is also not observed, because the peak value of the Hanle signal matches with the nonlocal spin-valve signal). That the mobile spins in the Si channel do not experience any significant exchange or magnetostatic stray field can be understood by considering that those fields originate from the magnetic tunnel contacts and are short range [33,43], and that the mobile electrons spent very little time in close proximity to the tunnel interfaces of the contacts while diffusing in the Si channel.
- [46] In principle, the electrons confined at the Si/MgO interface of the detector contact can acquire a spin accumulation by virtue of a coupling to the delocalized spins in the Si channel, which are spin polarized due to the spin current from the injector contact. However, the broad nonlocal Hanle signal that this would produce, if any, would depend on whether the magnetization of the injector and the detector are aligned P or AP.
- [47] M. Johnson and R. H. Silsbee, Calculation of nonlocal baseline resistance in a quasi-one-dimensional wire, *Phys. Rev. B* **76**, 153107 (2007).
- [48] F. Casanova, A. Sharoni, M. Erekhinsky, and I. K. Schuller, Control of spin injection by direct current in lateral spin valves, *Phys. Rev. B* **79**, 184415 (2009).
- [49] F. L. Bakker, A. Slachter, J.-P. Adam, and B. J. van Wees, Interplay of Peltier and Seebeck Effects in Nanoscale Nonlocal Spin Valves, *Phys. Rev. Lett.* **105**, 136601 (2010).
- [50] S. Kasai, S. Hirayama, Y. K. Takahashi, S. Mitani, K. Hono, H. Adachi, J. Ieda, and S. Maekawa, Thermal engineering of non-local resistance in lateral spin valves, *Appl. Phys. Lett.* **104**, 162410 (2014).
- [51] K. S. Das, F. K. Dejene, B. J. van Wees, and I. J. Vera-Marun, Anisotropic Hanle line shape via magnetothermoelectric phenomena, *Phys. Rev. B* **94**, 180403(R) (2016).
- [52] The nonlocal offset voltage is defined as the voltage that, when subtracted from the raw data, makes the nonlocal spin-valve data symmetric about the voltage axis, with the nonlocal voltages for the P and AP states having equal magnitude but opposite polarity, as expected for an ideal device with zero offset.
- [53] Note that this statement does not apply when the nonuniform current distribution in the channel is caused by the use of transparent or low resistance tunnel contacts. As shown in Ref. [47], in that case the current distribution depends explicitly on the ratio of the sheet resistance of the channel and the tunnel resistance of the injector contact, and the latter changes when the external field changes the spin accumulation, even if the current is kept constant.
- [54] J. Flipse, F. L. Bakker, A. Slachter, F. K. Dejene, and B. J. van Wees, Direct observation of the spin-dependent Peltier effect, *Nature Nanotech.* **7**, 166 (2012).

- [55] G. E. W. Bauer, E. Saitoh, and B. J. van Wees, Spin caloritronics, *Nature Mater.* **11**, 391 (2012).
- [56] J. C. Le Breton, S. Sharma, H. Saito, S. Yuasa, and R. Jansen, Thermal spin current from a ferromagnet to silicon by Seebeck spin tunnelling, *Nature* **475**, 82 (2011).
- [57] In the nonlocal measurements presented here, the bias polarity corresponds to the injection of electrons into the Si channel, and for this polarity, the narrow Hanle voltage across the injector contact is small because of the nonlinearity of spin detection in a biased magnetic tunnel contact (see Ref. [23]).
- [58] The ferromagnetic contacts were chosen to be smaller than the width of the Si channel strip so the magnetic tunnel contacts are not near the edges of the Si strip and critical mask alignment in the lithography process is avoided.